



Using GPS Radio Occultation to Monitor Sporadic-E

***8th International Radio Occultation Working Group Meeting
April 2021***



**Maj Dan Emmons - AFIT
Lt Rodney Carmona - AFIT
Dawn Merriman - AFIT
Lt Col Omar Nava - HAF
Eugene Dao - AFRL**

- Current global sporadic-E climatology
- Comparison of GPS radio occultation and ionosonde rates

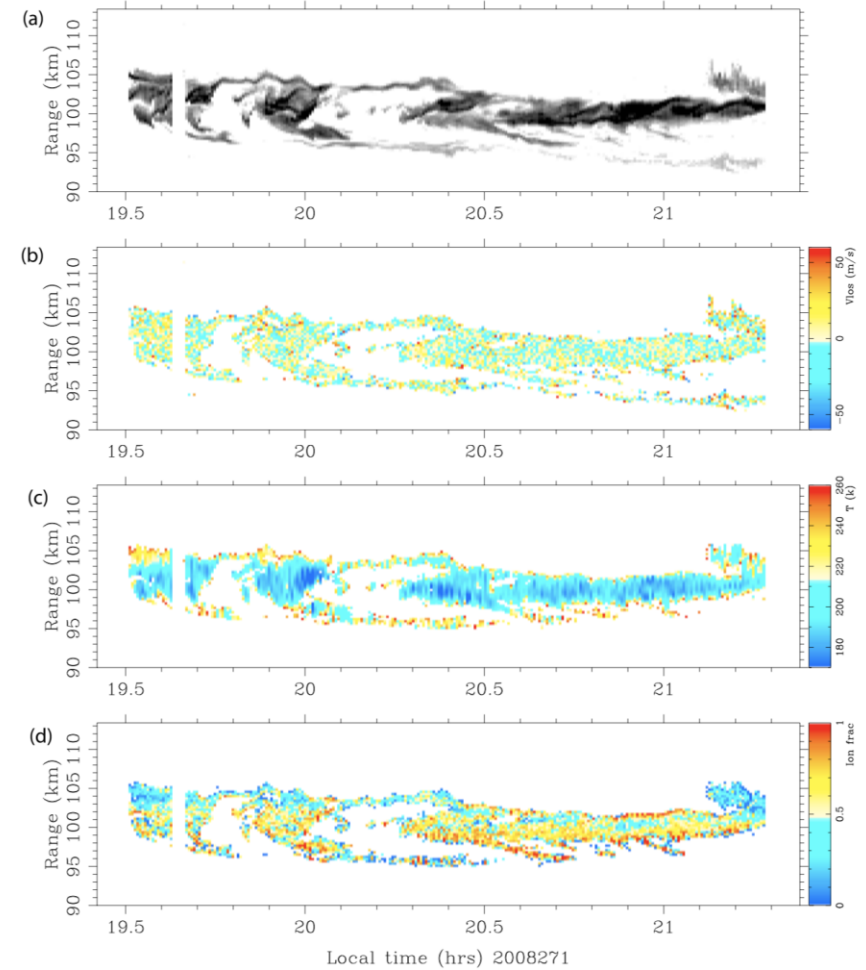
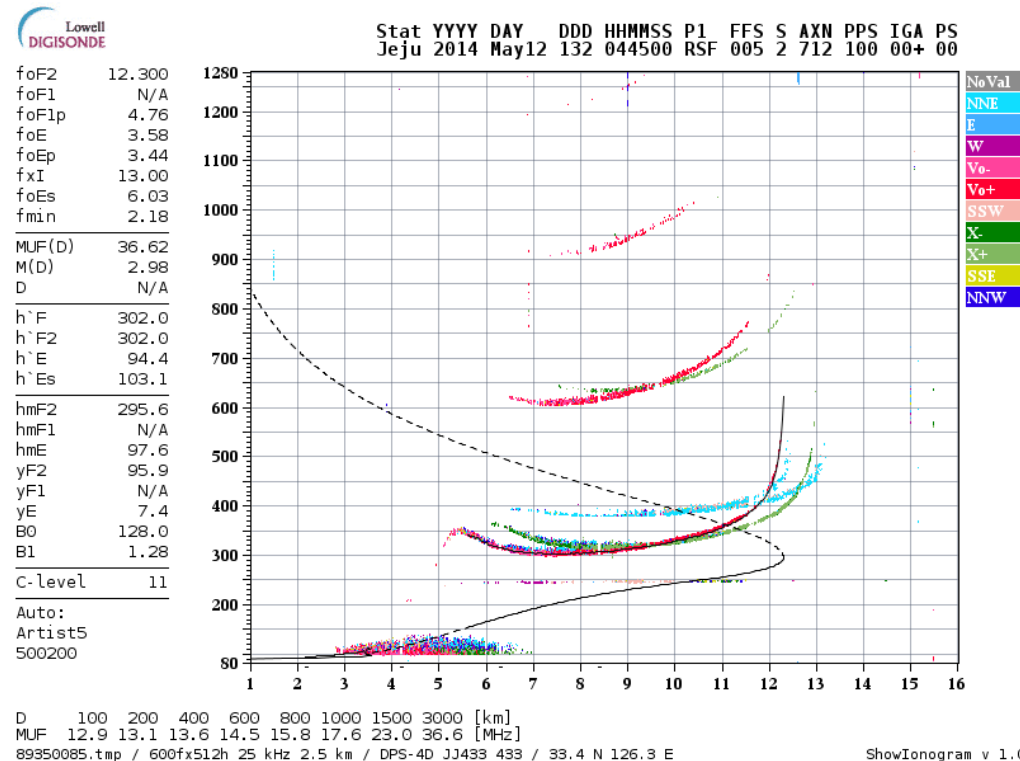
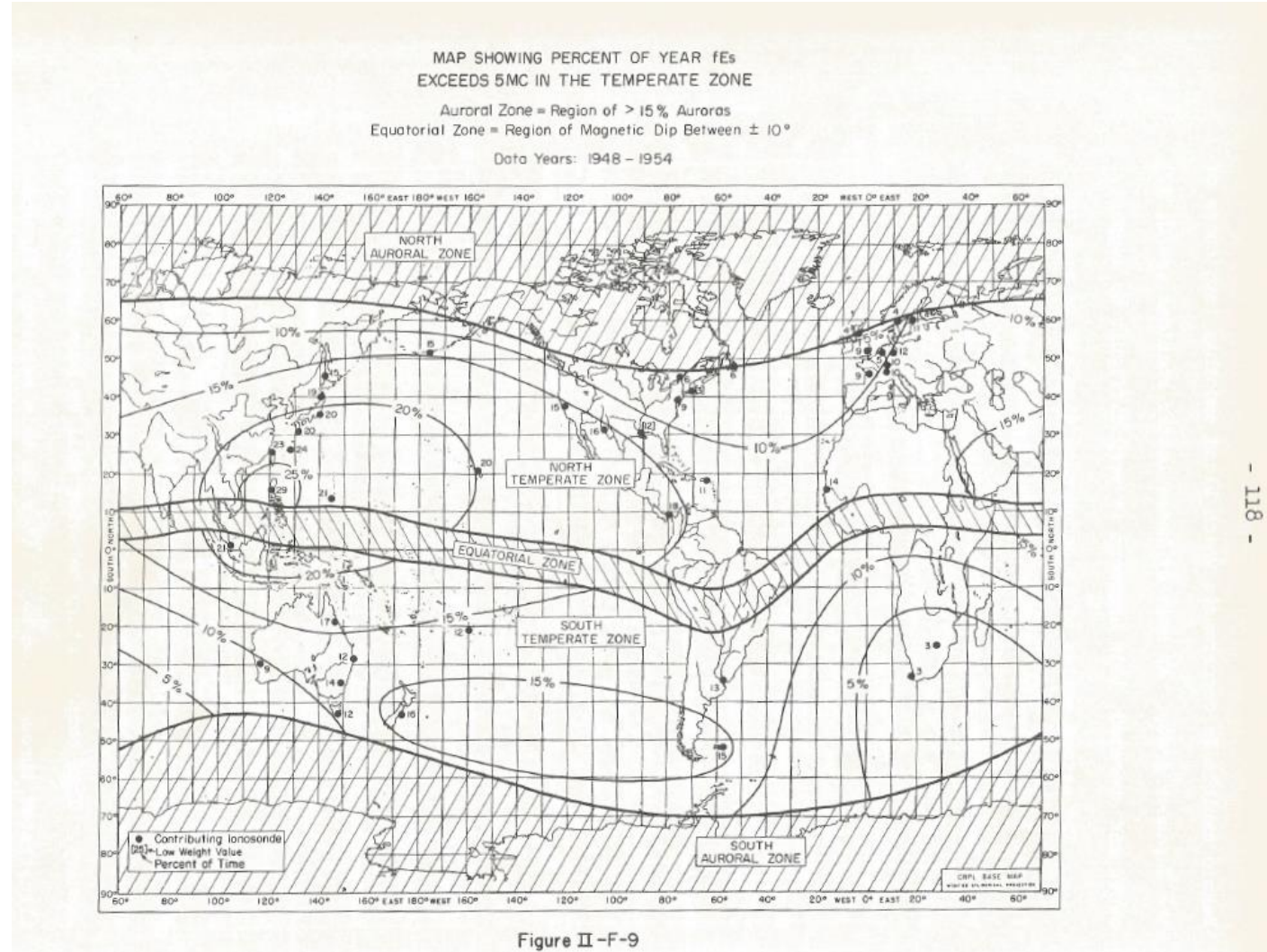


Figure 3. Sporadic *E* ionization layer observations made with the Arecibo incoherent scatter radar zenith-pointing line feed on September 27, 2008. (a) Relative density obtained from the magnitude of the first lag of the coded long pulse experiment. (b) Line-of-sight drifts. Red (blue) hues denote red (blue) shifts. (c) Temperature estimates. (d) Heavy metallic ion fraction estimates.

Current E_s Climatology: Ionosondes

- Smith provided the first global view of sporadic-E in the 1950's
- Climatology based primarily on ionosonde measurements
- Limited measurements over oceans, etc.
- These occurrence rates remain widely used today



Current E_s Climatology: Radio Occultation

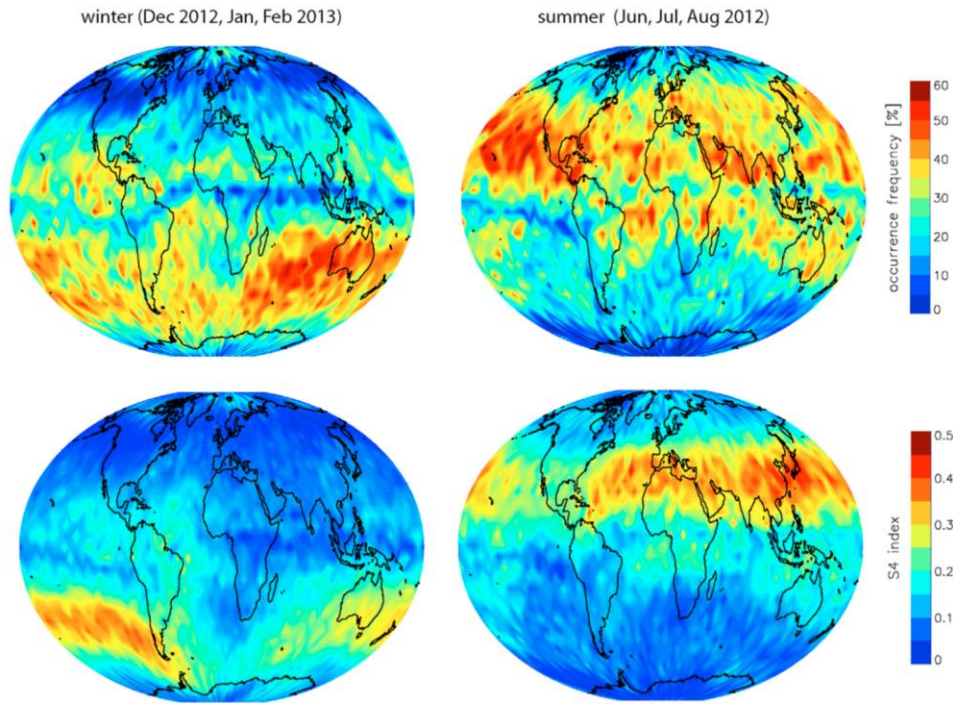


Fig. 3. Global distribution of sporadic E occurrence (upper row) and sporadic E intensity (lower row) for northern winter (left column) and northern summer (right column) conditions. The plots are produced from 3-monthly means centered around July 2012 and January 2013. They have a latitude/longitude resolution of $5^\circ \times 5^\circ$.

[Arras and Wickert, 2018]

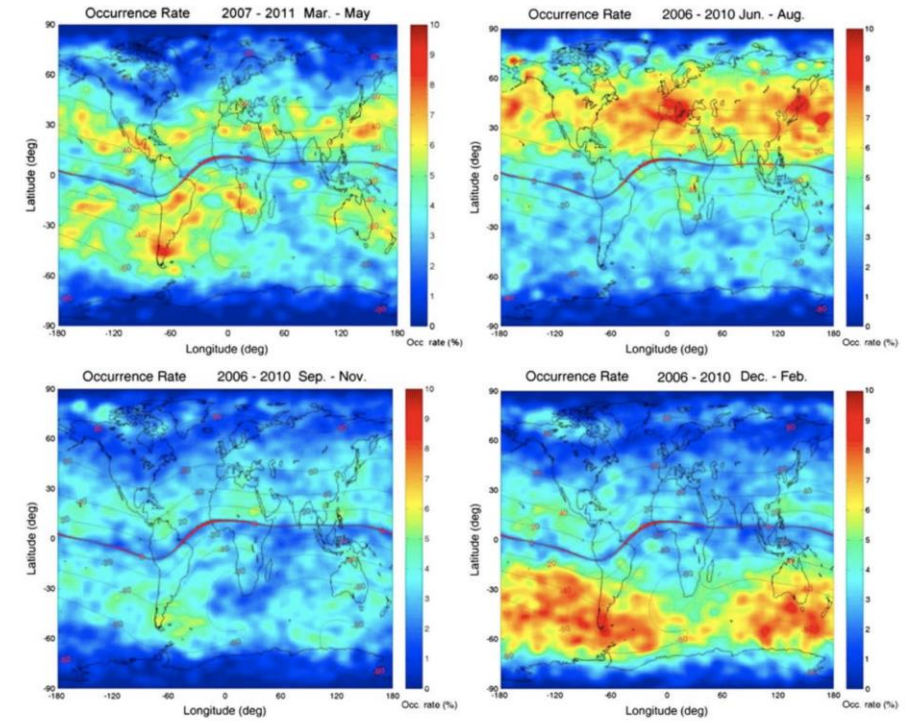


Figure 6. Occurrence rate of COSMIC-retrieved E_s layer for different seasons. Thin curves signify geomagnetic latitude contours and the thick curve is the geomagnetic equator.

[Chu et al., 2014]

- GPS-RO provides global coverage of E_s
- However, analysis of RO signals is non-trivial and current E_s occurrence rate estimates vary by a factor of ~ 5
- Need a way to validate GPS-RO occurrence rates: comparison with ionosondes

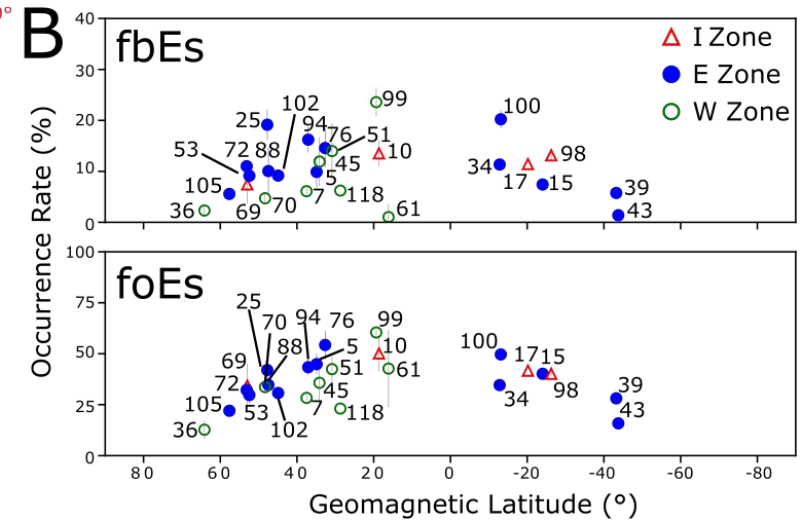
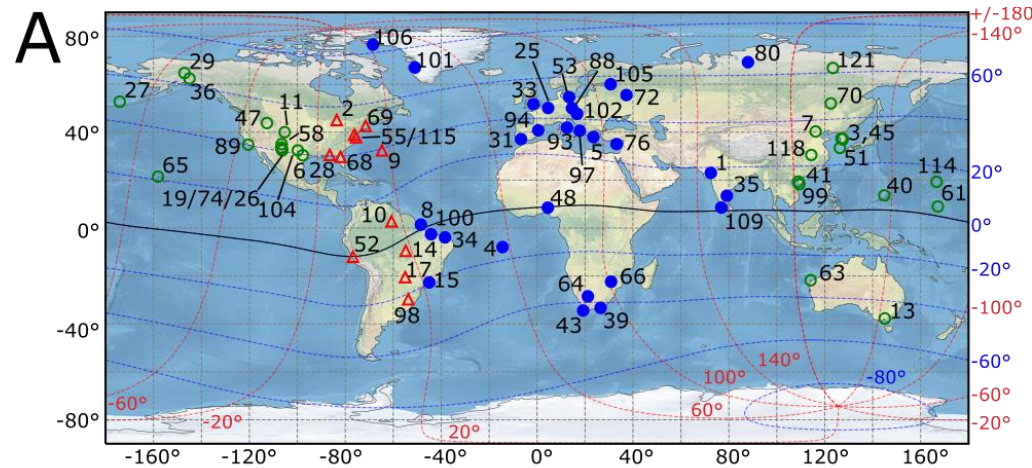


Updated Ionosonde Occurrence Rates



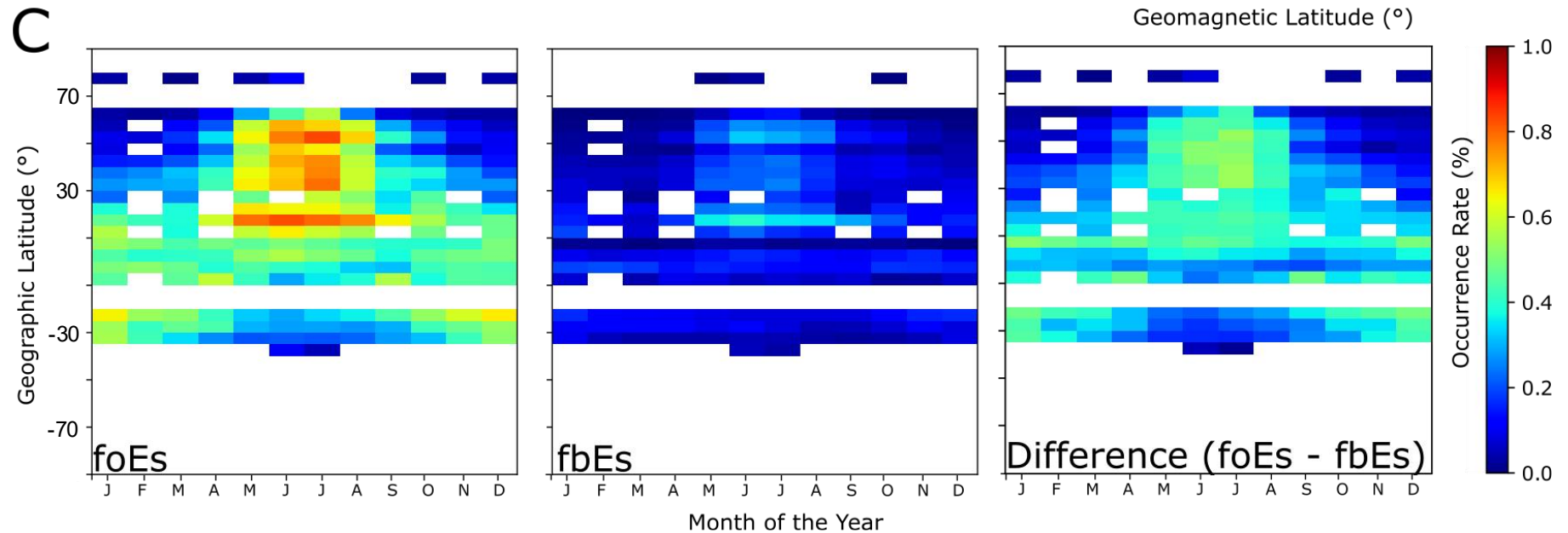
foEs or fbEs > 3 MHz

(A) Map of Digisonde sites with ARTIST5 data used in analysis



(B) Occurrence rates as a function of geomagnetic latitude: all seasons

(C) Monthly foEs and fbEs averages as a function of geographic latitude



- Current global sporadic-E climatology
- Comparison of GPS radio occultation and ionosonde rates

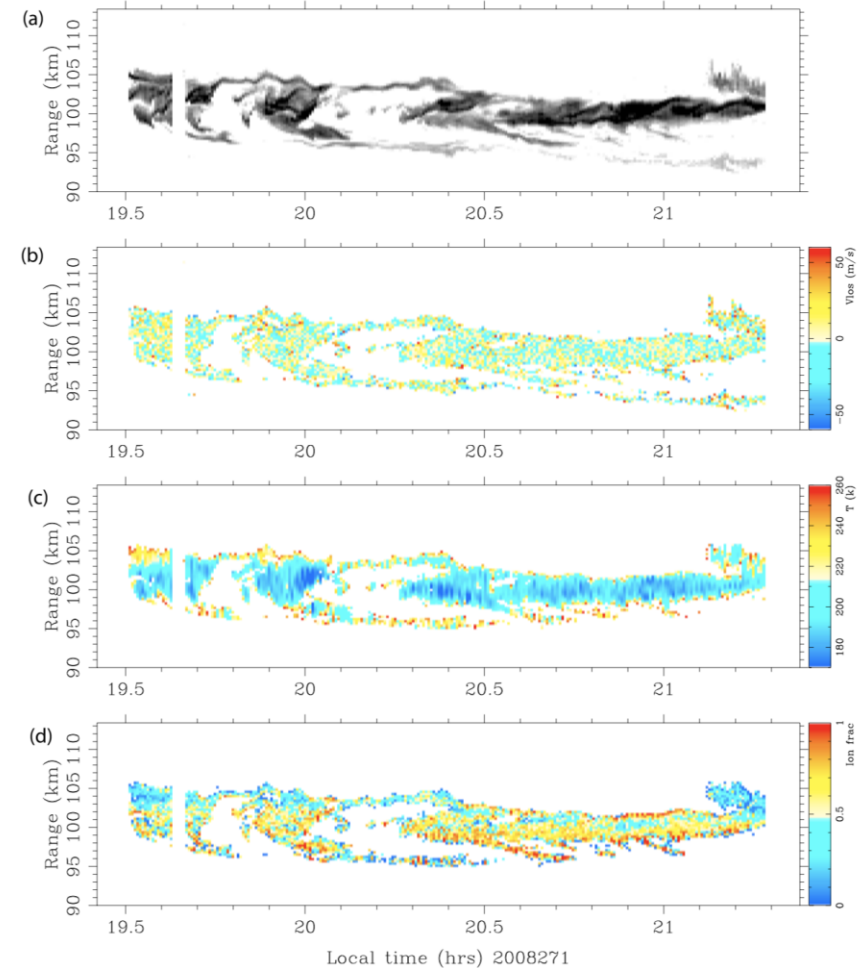
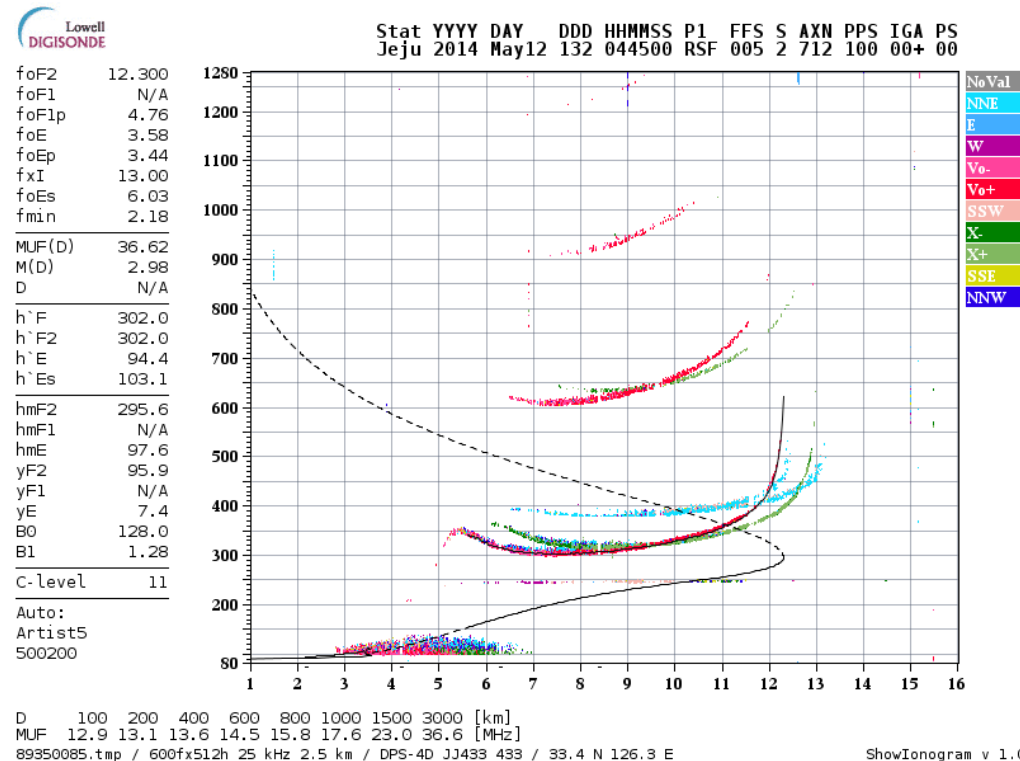


Figure 3. Sporadic *E* ionization layer observations made with the Arecibo incoherent scatter radar zenith-pointing line feed on September 27, 2008. (a) Relative density obtained from the magnitude of the first lag of the coded long pulse experiment. (b) Line-of-sight drifts. Red (blue) hues denote red (blue) shifts. (c) Temperature estimates. (d) Heavy metallic ion fraction estimates.

GPS-RO Techniques

- Five GPS-RO based techniques for monitoring sporadic-E are compared using COSMIC-1 measurements from 2010-2017 (<https://cdaac-www.cosmic.ucar.edu/>)
- Binary threshold either defined by initial study or calculated fbEs > 3.0 MHz
 - Note: GPS-RO measures fb μ Es (Haldoupis, 2019)

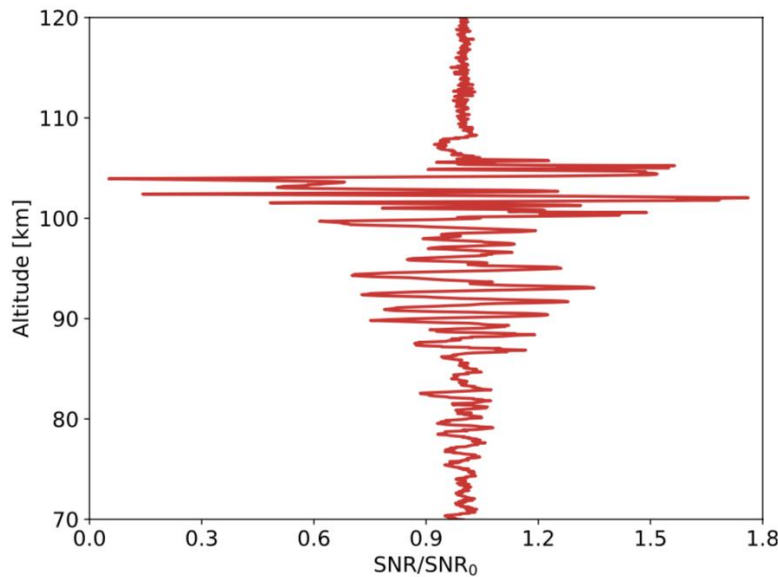


Fig. 5. An example of the normalized SNR for the L1 signal as a function of altitude. The characteristic u-shape used to calculate the sporadic-E cloud thickness is present near 103 km.

[Gooch, 2020]

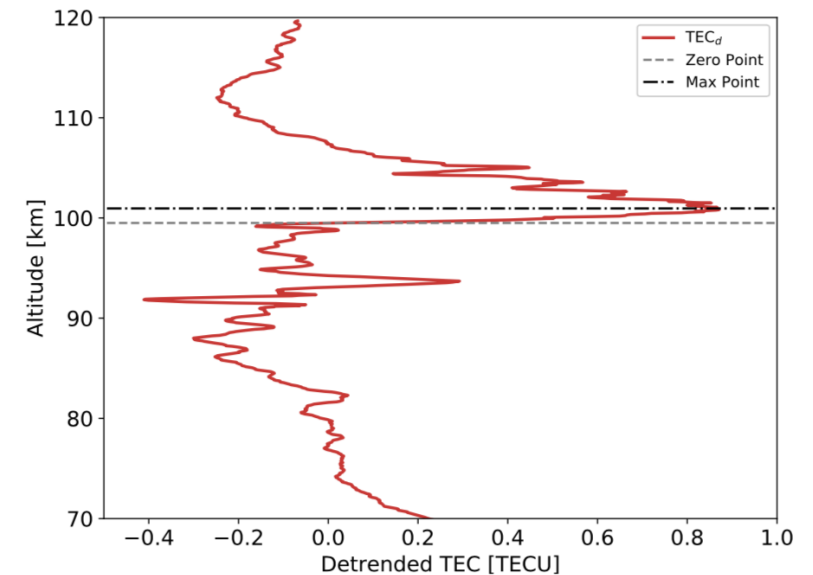
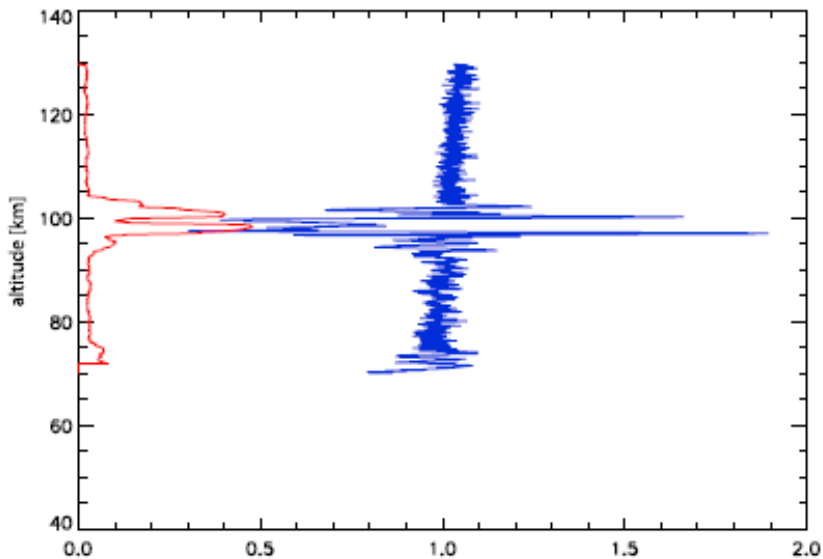


Fig. 3. An example of the detrended TEC, TEC_d , used to calculate the altitudes corresponding to the TEC perturbation, ΔTEC , caused by a sporadic-E layer. The dash-dot line corresponds to the altitude of peak TEC_d while the dashed line is associated with the first zero point below the peak (base).

GPS-RO Techniques

- Yu et al. (2020) technique:
 - Based on 1 Hz S_4 calculation
 - Derived from a global fit to ionosonde data

$$(foEs - 1.2)^2 = 13.62 \times S_{4,Max}$$



normalized SNR, standard deviation

[Arras and Wickert, 2018]

- Chu et al. (2014) technique:
 - 1 Hz sampling rate (ionPhs from CDAAC)
 - Three criteria must be satisfied simultaneously:
 1. L_1 and L_2 phase perturbations must exceed 5 cm
 2. Excess phase ratio of ΔL_2 to ΔL_1 within 1.5-1.8
 3. Amplitude of normalized L_1 SNR perturbation greater than 0.01
- Arras and Wickert (2018) technique:
 - 50 Hz L_1 SNR (atmPhs from CDAAC) data
 - Empirically determined standard deviation threshold of 0.2 within 10 km altitude range



GPS-RO Techniques

- Niu et al. (2019) technique:

- 1 Hz L₁ and L₂ phase data
- Background TEC (TEC_b) calculated using an 11-point low-pass filter

$$TEC(z) = TEC_b(z) + \Delta TEC(z)$$

- S-index is vertical gradient of the TEC perturbation

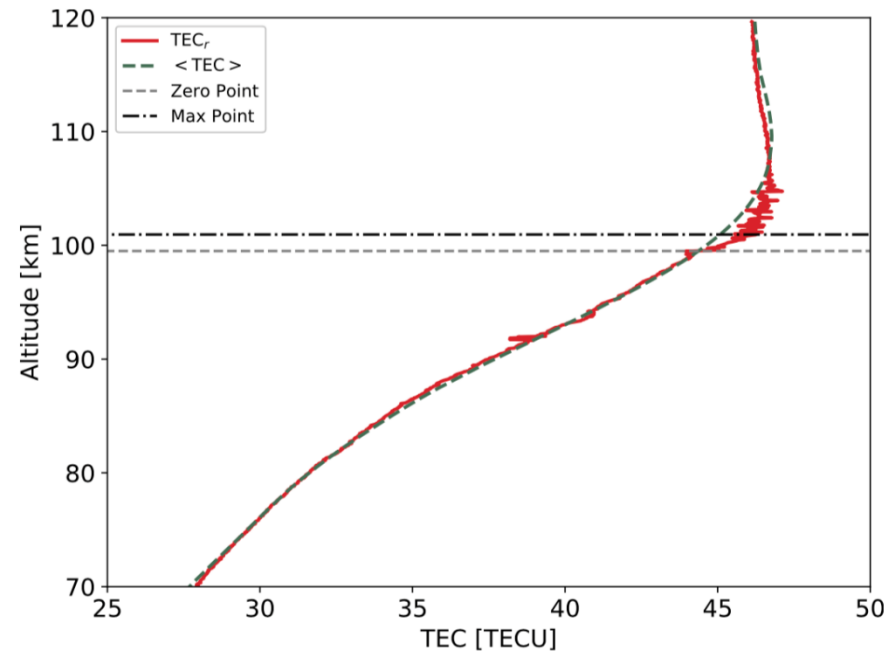
$$S = \frac{d(\Delta TEC)}{dz}$$

- S_{max} = maximum S-index in E-region

$$S_{\max} \left[\frac{\text{TECU}}{\text{km}} \right] = 0.0502 \text{ foEs}[\text{MHz}] - 0.0304$$

- Gooch et al. (2020)

- 50 Hz L₁ and L₂ phase data
- Calculate slowly varying background TEC (<TEC>) using a Savitzky-Golay filter with a 25 km window
- Detrend TEC and convert to n_e

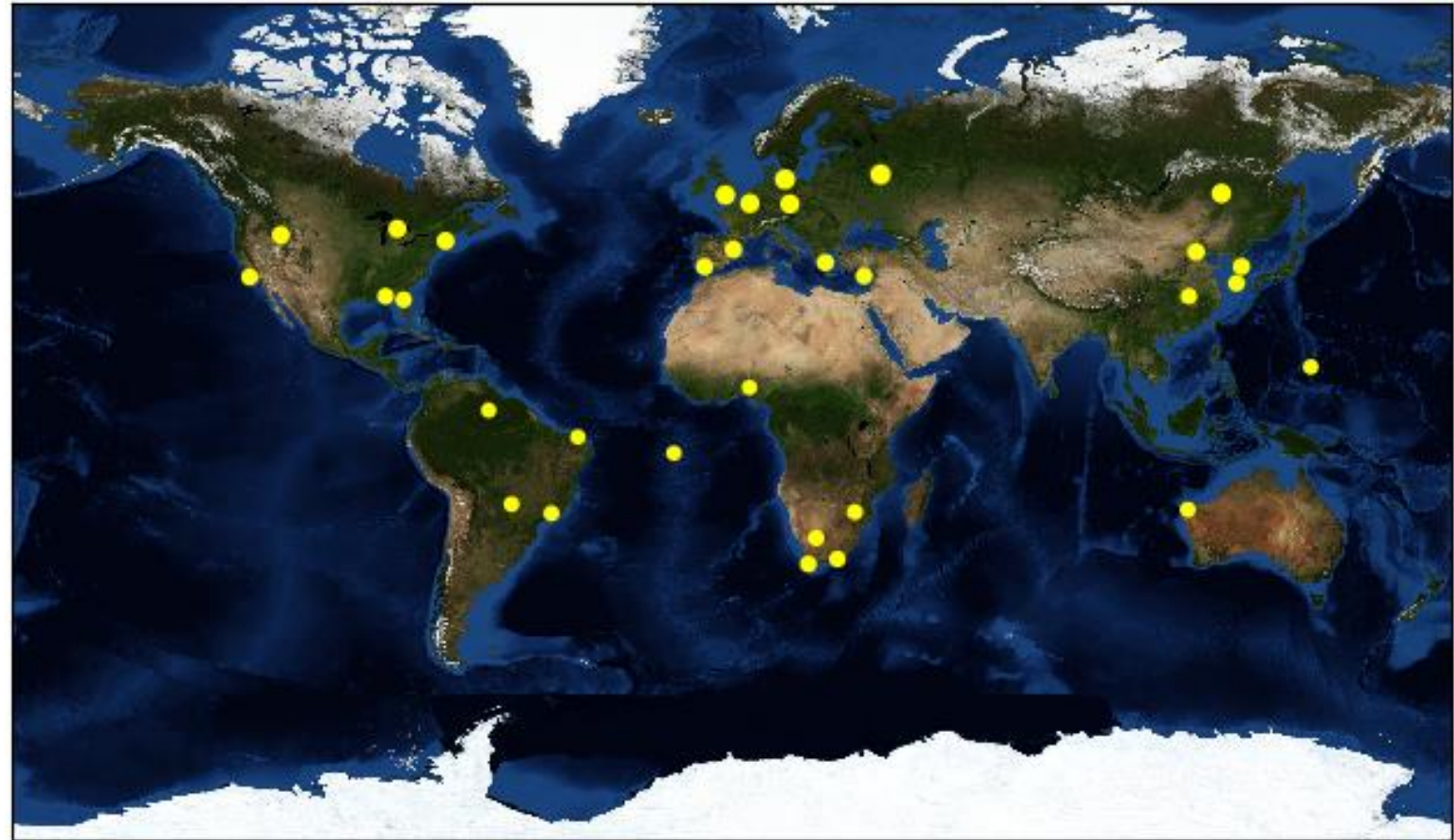


[Gooch et al., 2020]

$$\Delta n_e \sim \frac{(TEC - \langle TEC \rangle)}{(2\sqrt{2r\Delta r})}$$

Comparison Criteria

- Count number of RO tangent points with 100 km altitude within 170 km (average length of sporadic-E: Cathey, 1969) of each Digisonde site
- Use the binary sporadic-E thresholds for each GPS-RO technique to count the number of occurrences for each site
- Separate the occurrence rates by season and compare to Digisonde rates

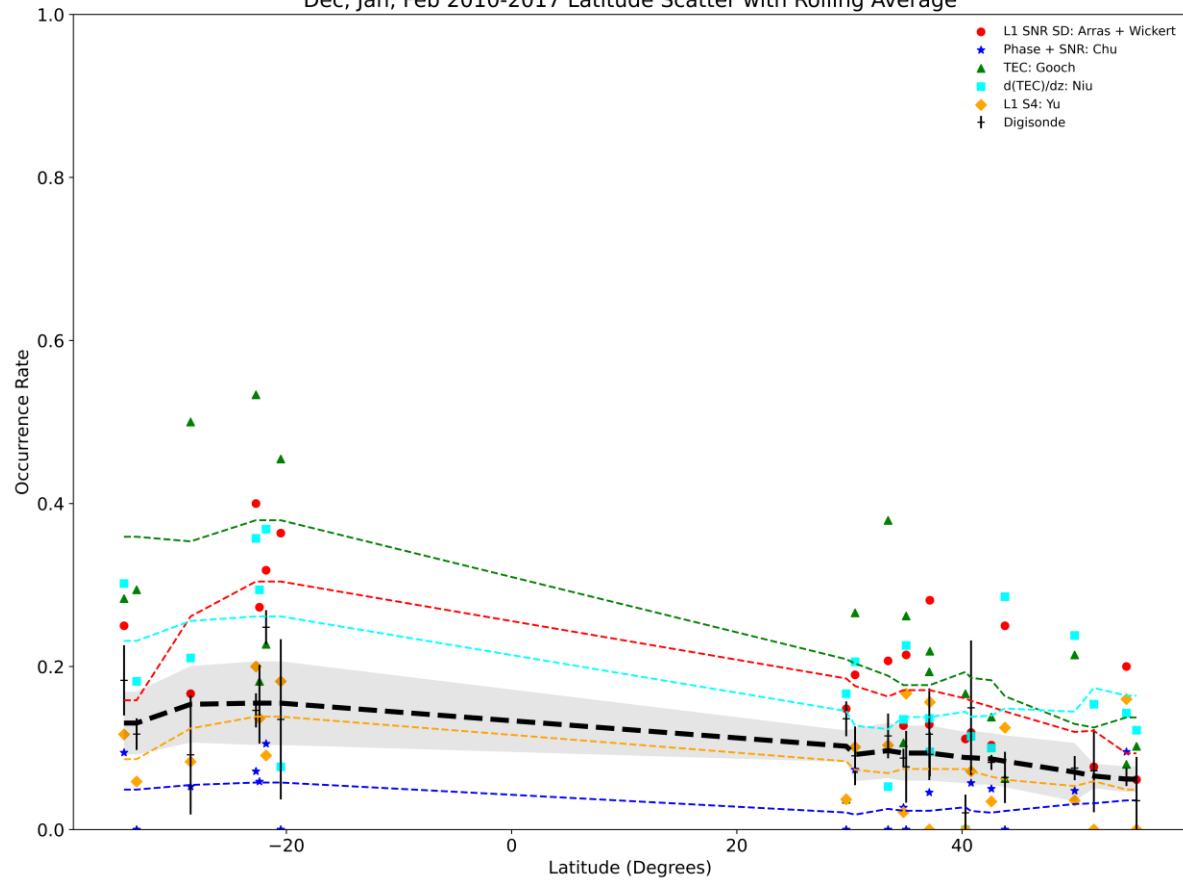




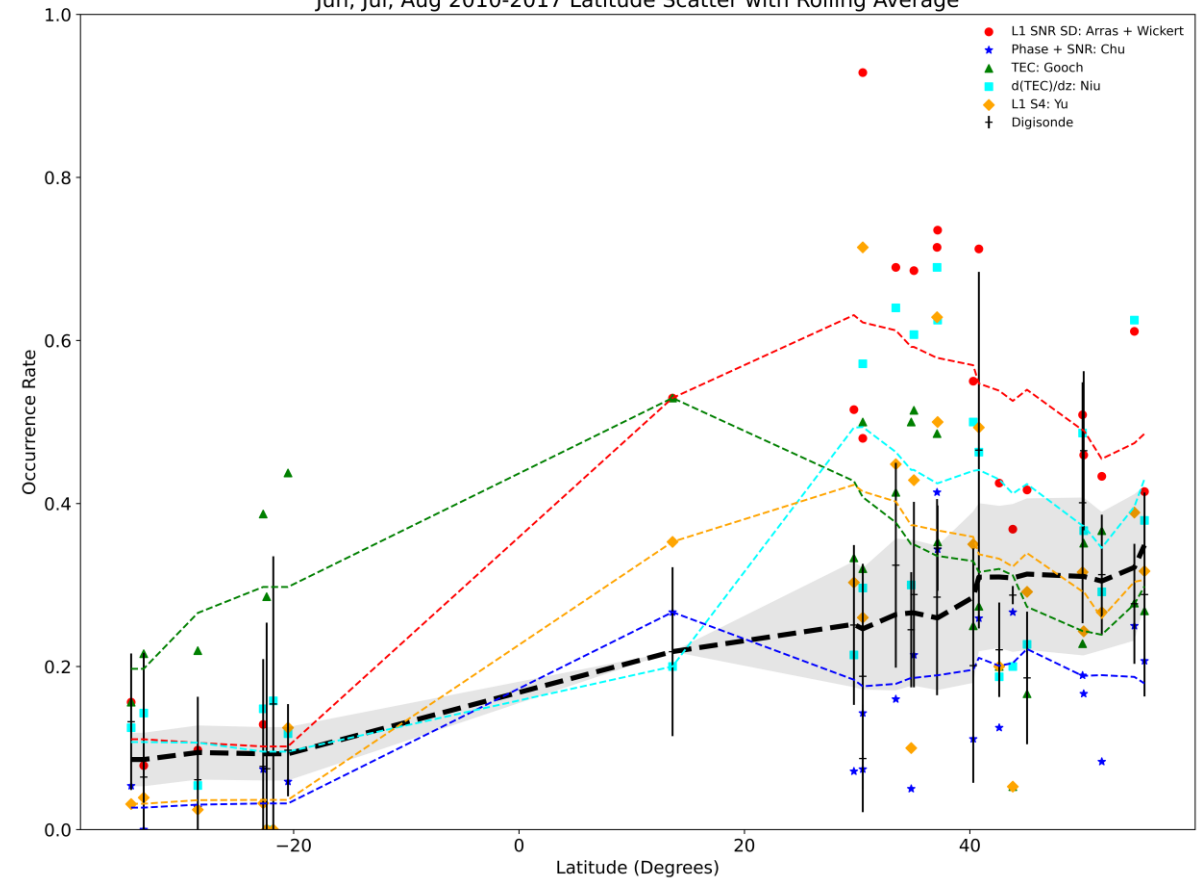
Results: Summer and Winter



Dec, Jan, Feb 2010-2017 Latitude Scatter with Rolling Average

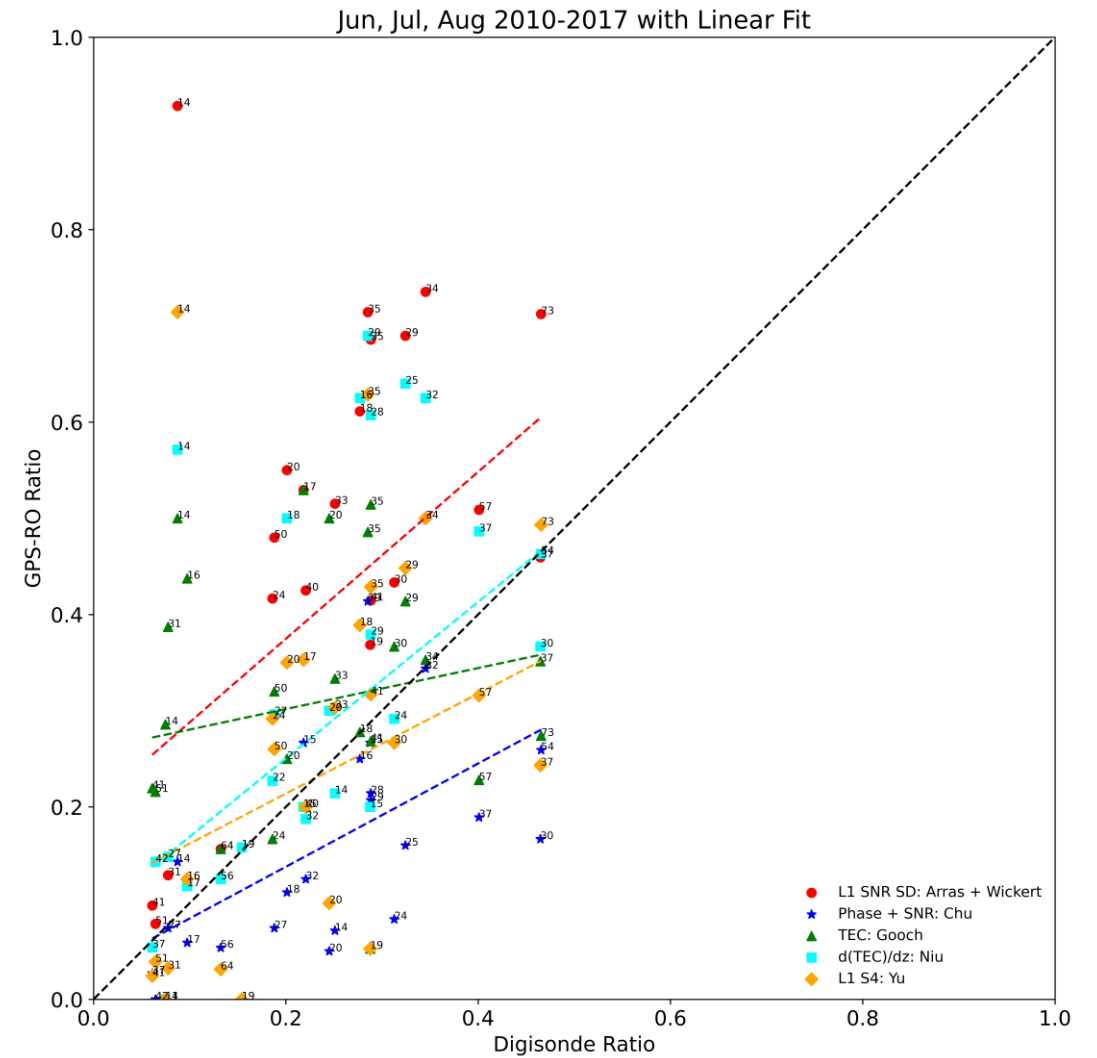
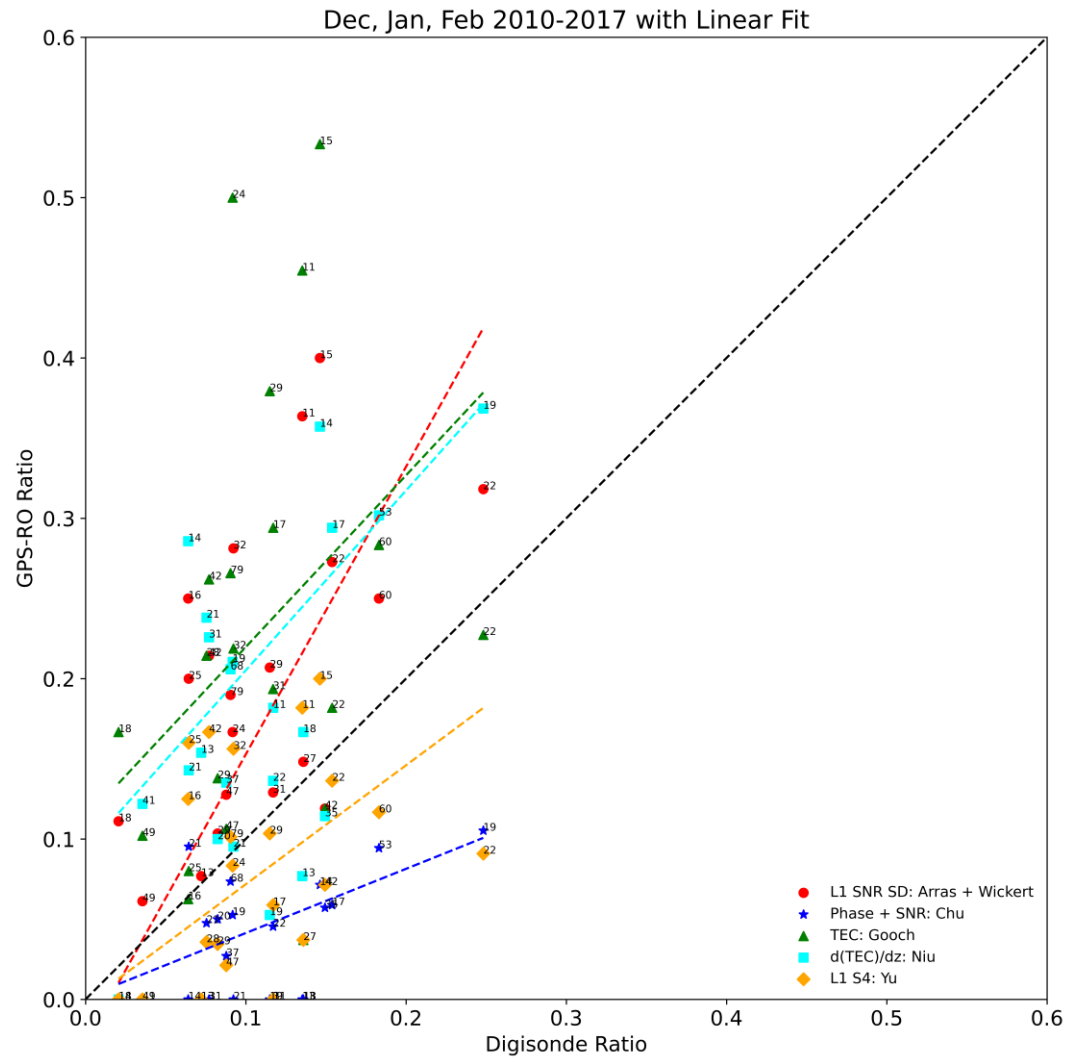


Jun, Jul, Aug 2010-2017 Latitude Scatter with Rolling Average





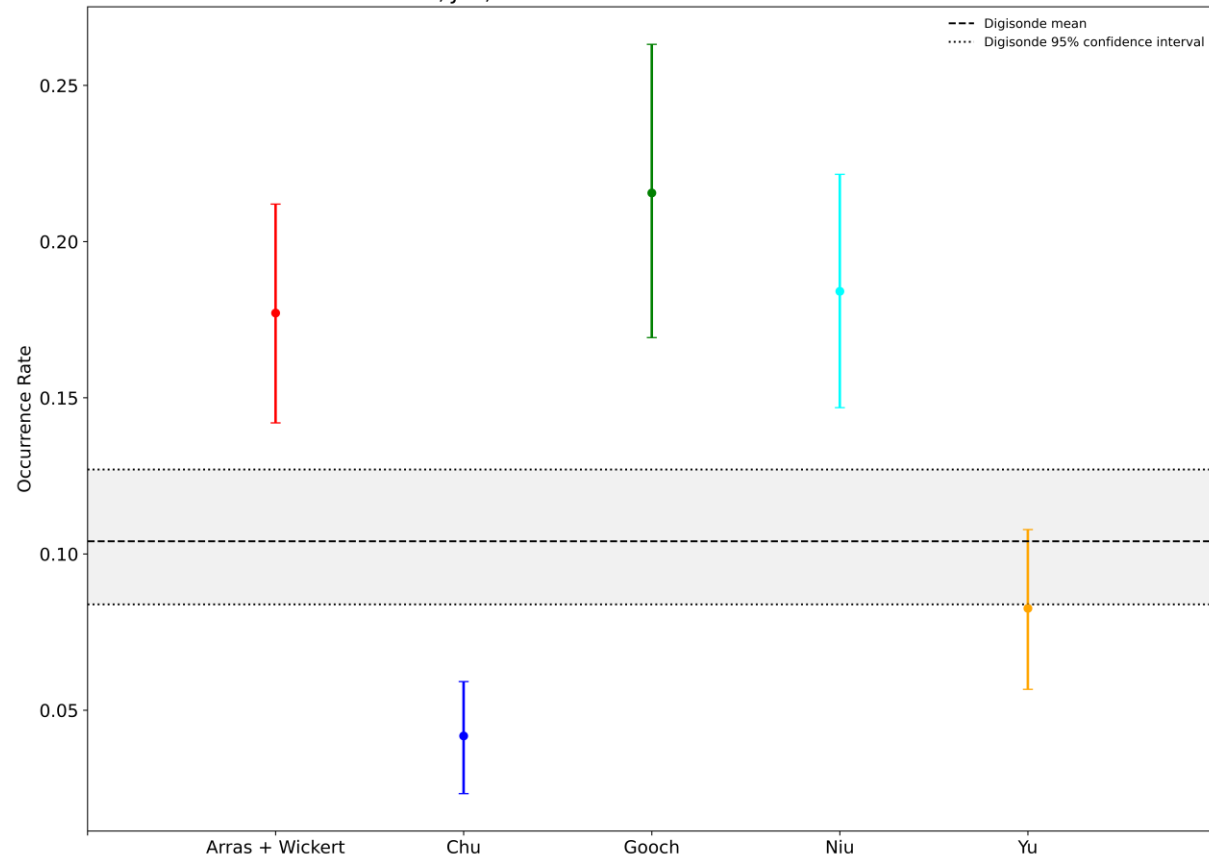
Occurrence Rates: Linear Fit



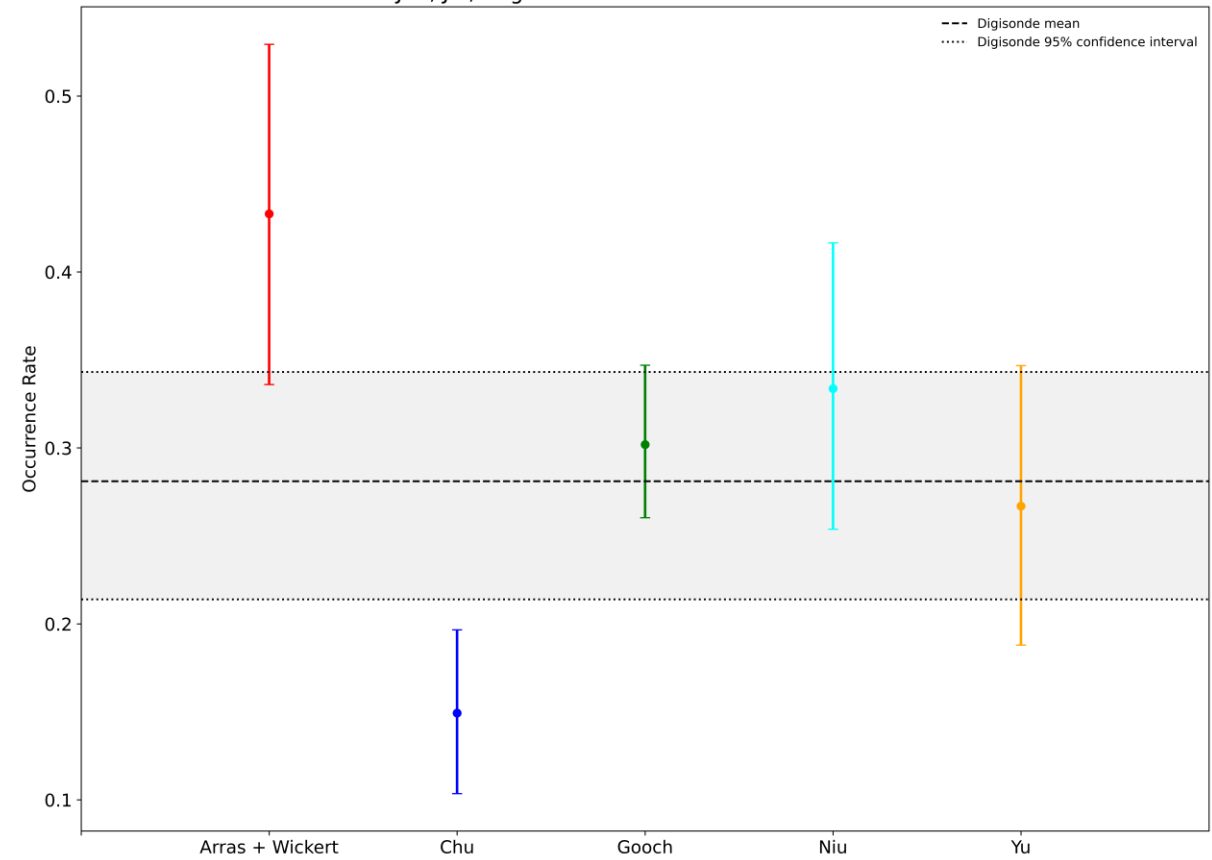


Bootstrapping Means

Dec, Jan, Feb 2010-2017 Mean Occurrence Rate



Jun, Jul, Aug 2010-2017 Mean Occurrence Rate





Conclusions

- ARTIST-5 autoscaling of Digisonde ionograms provides the “ground-truth” for sporadic-E foEs and fbEs occurrence rates
- Limited number of ionosonde sites make global occurrence rate calculations difficult: need to include GPS-RO data
- Overall, the Yu et al. (2020) S_4 GPS-RO technique showed the closest agreement with ionosonde measurements during the span of 2010-2017
- Next step: use the S_4 technique in combination with Digisonde data to develop an updated global climatology



Questions?



foF2 N/A
 foF1 N/A
 foF1p 4.35
 foE 3.32
 foEp 3.24
 fxI N/A
 foEs 8.93
 fmin 2.00

MUF(D) N/A
 M(D) N/A
 D N/A

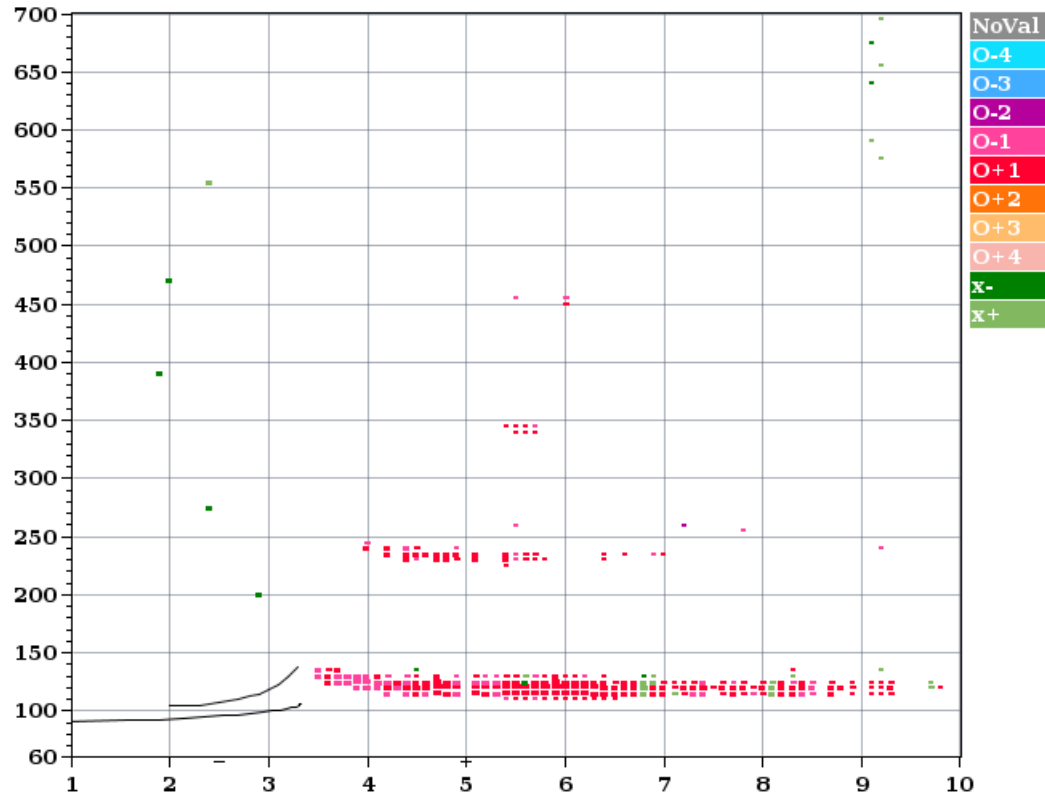
h`F N/A
 h`F2 N/A
 h`E 105.5
 h`Es 123.1

hmF2 N/A
 hmF1 N/A
 hmE 106.6
 yF2 N/A
 yF1 N/A
 yE 16.2
 B0 N/A
 B1 N/A

C-level N/A

Manual:
 David
 Altadill

Station YYYY DAY DDD HHMMSS P1 FFS S AXN PPS IGA PS
 ROQUETES 2010 Jun09 160 114505 MMM 1 046 100 31+ 11



D 100 200 400 600 800 1000 1500 3000 [km]
 MUF 0.0 0.0 0.0 0.0 0.0 0.0 0.0 0.0 [MHz]
 30907797.tmp / 90fx128h 100 kHz 5.0 km / DGS-256 EB040 041 / 40.8 N 0.5 E

ShowIonogram v 1.0



References

1. Hysell, D. L., Nossa, E., Larsen, M. F., Munro, J., Sulzer, M. P., & González, S. A. (2009). Sporadic E layer observations over Arecibo using coherent and incoherent scatter radar: Assessing dynamic stability in the lower thermosphere. *Journal of Geophysical Research: Space Physics*, 114(A12).
2. Smith, E. K. (1957). Worldwide occurrence of sporadic E (Vol. 582). US Department of Commerce, National Bureau of Standards.
3. Arras, C., & Wickert, J. (2018). Estimation of ionospheric sporadic E intensities from GPS radio occultation measurements. *Journal of Atmospheric and Solar-Terrestrial Physics*, 171, 60-63.
4. Chu, Y. H., Wang, C. Y., Wu, K. H., Chen, K. T., Tzeng, K. J., Su, C. L., Feng, W., Plane, J. M. C. (2014). Morphology of sporadic E layer retrieved from COSMIC GPS radio occultation measurements: Wind shear theory examination. *Journal of Geophysical Research: Space Physics*, 119(3), 2117-2136.
5. Haldoupis, C. (2019). An Improved Ionosonde-Based Parameter to Assess Sporadic E Layer Intensities: A Simple Idea and an Algorithm. *Journal of Geophysical Research: Space Physics*, 124(3), 2127-2134.
6. Cathey, E. H. (1969). Some midlatitude sporadic-E results from the Explorer 20 satellite. *Journal of Geophysical Research*, 74(9), 2240-2247.
7. Niu, J., Weng, L. B., Meng, X., & Fang, H. X. (2019). Morphology of Ionospheric Sporadic E Layer Intensity Based on COSMIC Occultation Data in the Midlatitude and Low-Latitude Regions. *Journal of Geophysical Research: Space Physics*, 124(6), 4796-4808.
8. Gooch, J. Y., Colman, J. J., Nava, O. A., & Emmons, D. J. (2020). Global ionosonde and GPS radio occultation sporadic-E intensity and height comparison. *Journal of Atmospheric and Solar-Terrestrial Physics*, 199, 105200.
9. Yu, B., Scott, C. J., Xue, X., Yue, X., & Dou, X. (2020). Derivation of global ionospheric Sporadic E critical frequency (fo Es) data from the amplitude variations in GPS/GNSS radio occultations. *Royal Society open science*, 7(7), 200320.